

SELF-SUPERVISED DATASET DISTILLATION FOR TRANSFER LEARNING

Dong Bok Lee^{1*}, Seanie Lee^{1*}, Joonho Ko¹ Kenji Kawaguchi², Juho Lee¹, Sung Ju Hwang¹

KAIST¹, National University of Singapore²

{markhi, lsnfamily02, joonho.ko, juholee sjhwang82}@kaist.ac.kr
kenji@comp.nus.edu.sg

ABSTRACT

Dataset distillation methods have achieved remarkable success in distilling a large dataset into a small set of representative samples. However, they are not designed to produce a distilled dataset that can be effectively used for facilitating self-supervised pre-training. To this end, we propose a novel problem of distilling an unlabeled dataset into a set of small synthetic samples for efficient self-supervised learning (SSL). We first prove that a gradient of synthetic samples with respect to a SSL objective in naive bilevel optimization is *biased* due to the randomness originating from data augmentations or masking. To address this issue, we propose to minimize the mean squared error (MSE) between a model’s representations of the synthetic examples and their corresponding learnable target feature representations for the inner objective, which does not introduce any randomness. Our primary motivation is that the model obtained by the proposed inner optimization can mimic the *self-supervised target model*. To achieve this, we also introduce the MSE between representations of the inner model and the self-supervised target model on the original full dataset for outer optimization. Lastly, assuming that a feature extractor is fixed, we only optimize a linear head on top of the feature extractor, which allows us to reduce the computational cost and obtain a closed-form solution of the head with kernel ridge regression. We empirically validate the effectiveness of our method on various applications involving transfer learning.

1 INTRODUCTION

As a consequence of collecting large-scale datasets and recent advances in parallel data processing, deep models have achieved remarkable success in various machine learning problems. However, some applications such as hyperparameter optimization (Franceschi et al., 2017), continual learning (Lopez-Paz & Ranzato, 2017), or neural architecture search (Liu et al., 2019) require repetitive training processes. In such scenarios, it is prohibitively costly to use all the examples from the huge dataset, which motivates the need to compress the full dataset into a small representative set of examples. Recently, many dataset distillation (or condensation) methods (Wang et al., 2018; Zhao et al., 2021; Zhao & Bilen, 2021; Nguyen et al., 2021a;b; Cazenavette et al., 2022; Zhou et al., 2022; Loo et al., 2022; Zhao & Bilen, 2023) have successfully learned a small number of examples on which we can train a model to achieve performance comparable to the one trained on the full dataset.

Despite the recent success of dataset distillation methods, they are not designed to produce a distilled dataset that can be effectively transferred to downstream tasks (Figure 1-(a)). In other words, we may not achieve meaningful performance improvements when pre-training a model on the distilled dataset and fine-tuning it on the target dataset. However, condensing general-purpose datasets into a small set for transfer learning is crucial for some applications. For example, instead of using a large pre-trained model, we may need to search a hardware-specific neural architecture due to constraints on the device (Lee et al., 2021). To evaluate the performance of an architecture during the search process, we repeatedly pre-train a model with the architecture on large unlabeled dataset and fine-tune it on the target training dataset, which is time consuming and expensive. If we distill the pre-training dataset into a small dataset at once, we can accelerate the architecture search by

*Equal contribution

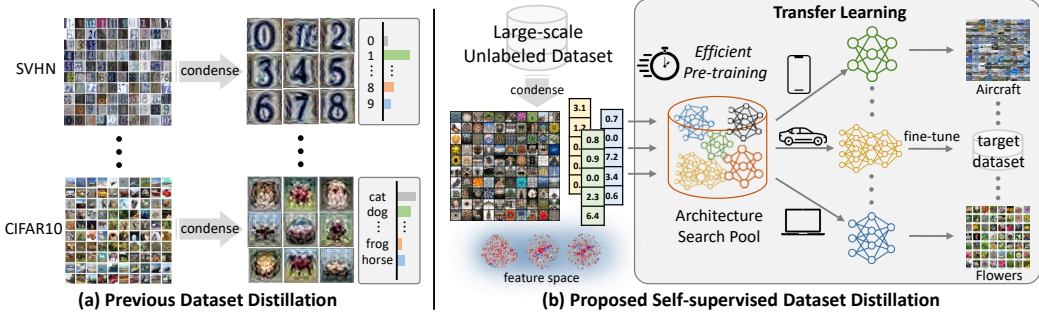


Figure 1: (a): Previous supervised dataset distillation methods. (b): Our proposed method that distills **unlabeled dataset** into a small set that can be effectively used for **pre-training and transferred** to target datasets.

pre-training the model on the small set. Another example is target data-free knowledge distillation (KD) (Lopes et al., 2017; Raikwar & Mishra, 2022), where we aim to distill a teacher into a smaller student without access to the target training data due to data privacy or intellectual property issues. Instead of the target dataset, we can employ a condensed surrogate dataset for KD (Kim et al., 2023).

To obtain a small representative set for efficient pre-training, as illustrated in Figure 1-(b), we propose a *self-supervised dataset distillation framework* which distills an unlabeled dataset into a small set on which the pre-training will be done. Specifically, we formulate the unsupervised dataset distillation as a bilevel optimization problem: optimizing a small representative set such that a model trained on the small set can induce a latent representation space similar to the space of the model trained on the full dataset. Naively, we can replace the objective function of existing bilevel optimization methods for supervised dataset condensation with a SSL objective function that involves some randomness, such as data augmentations or masking inputs. However, we have empirically found that back-propagating through data augmentation or masking is unstable. Moreover, we prove that a gradient of the self-supervised learning (SSL) loss with randomly sampled data augmentations or masking is *a biased estimator of the true gradient*, explaining the instability.

Based on this insight, we propose to use a mean squared error (MSE) for both inner and outer objective functions, which does not introduce any randomness due to the SSL objectives and thus contributes to stable optimization. First, we parameterize a pair of synthetic examples and target representations of the synthetic ones. For inner optimization, we train a model to minimize the MSE between the target representations and a model’s representations of the synthetic examples. Then, we evaluate the MSE between the original data representation of the model trained with the inner optimization and that of the model pre-trained on the original full dataset with a SSL objective. Since we do not sample any data augmentations or input masks, we can avoid the biased gradient of the SSL loss. Lastly, similar to Zhou et al. (2022), we simplify the inner optimization to reduce computational cost. We decompose the model into a feature extractor and a linear head, and optimize only the linear head with kernel ridge regression during the inner optimization while freezing the feature extractor. With the linear head and the frozen feature extractor, we compute the meta-gradient of the synthetic examples and target representations with respect to the outer loss, and update them. To this end, we dub our proposed self-supervised dataset distillation method for transfer learning as *Kernel Ridge Regression on Self-supervised Target (KRR-ST)*.

We empirically show that our proposed KRR-ST significantly outperforms the supervised dataset distillation methods in transfer learning experiments, where we condense a source dataset, which is either CIFAR100 (Krizhevsky et al., 2009), TinyImageNet (Le & Yang, 2015), or ImageNet (Deng et al., 2009), into a small set, pre-train models with different architectures on the condensed dataset, and fine-tune all the models on target labeled datasets such as CIFAR10, Aircraft (Maji et al., 2013), Stanford Cars (Krause et al., 2013), CUB2011 (Wah et al., 2011), Stanford Dogs (Khosla et al., 2011), and Flowers (Nilsback & Zisserman, 2008). Our contributions are as follows:

- We propose a new problem of *self-supervised dataset distillation* for transfer learning, where we distill an unlabeled dataset into a small set, pre-train a model on it, and fine-tune it on target tasks.
- We have observed training instability when utilizing existing SSL objectives in bilevel optimization for self-supervised dataset distillation. Furthermore, we prove that a gradient of the SSL objectives with data augmentations or masking inputs is *a biased estimator of the true gradient*.
- To address the instability, we propose **KRR-ST** using MSE without any randomness at an inner loop. For the inner loop, we minimize MSE between a model representation of synthetic samples

and target representations. For an outer loop, we minimize MSE between the original data representation of the model from inner loop and that of the model pre-trained on the original dataset.

- We extensively validate our proposed method on numerous target datasets and architectures, and show that ours outperforms supervised dataset distillation methods.

2 RELATED WORK

Dataset Distillation (or Condensation) To compress a large dataset into a small set, instead of selecting coresets (Borsos et al., 2020; Mirzasoleiman et al., 2020), dataset condensation optimizes a small number of synthetic samples while preserving information of the original dataset to effectively train high-performing deep learning models. Wang et al. (2018) propose the first dataset distillation (DD) method based on bilevel optimization, where the inner optimization is simply approximated by one gradient-step. Instead of one-step approximation, recent works propose a back-propagation through time for full inner optimization steps (Deng & Russakovsky, 2022), or implicit gradient based on implicit function theorem (Loo et al., 2023). This bilevel formulation, however, incurs expensive computational costs and hinders scaling to large datasets. To overcome this, several papers propose surrogate objective alternatives to bilevel optimization. Specifically, DSA (Zhao et al., 2021; Zhao & Bilen, 2021) minimizes the distance between gradients of original and synthetic samples for each training step. MTT (Cazenavette et al., 2022) proposes to match the parameter obtained on real data and the parameter optimized on the synthetic data. DM (Zhao & Bilen, 2023) matches the first moments of the feature distributions induced by the original dataset and synthetic dataset. As another line of work, Kernel Inducing Points (Nguyen et al., 2021a;b) propose DD methods based on kernel ridge regression, which simplifies inner optimization by back-propagating through Neural Tangent Kernel (NTK) (Lee et al., 2019). Due to the expensive cost of computing NTK for neural networks, FRePo (Zhou et al., 2022) proposes kernel ridge regression on neural features sampled from a pool, and RFAD (Loo et al., 2022) proposes random feature approximation of the neural network Gaussian process. Despite the recent advances in DD methods, none of them have tackled unsupervised DD for transferable learning.

Self-Supervised Learning A vast amount of works have proposed self-supervised learning (SSL) methods. A core idea of SSL is that we use large-scale unlabeled data to train a model to learn meaningful representation space that can be effectively transferred to downstream tasks. We introduce a few representative works. SimCLR (Chen et al., 2020a) is one of the representative contrastive learning methods. It maximizes the similarity between two different augmentations of the same input while minimizing the similarity between two randomly chosen pairs. MOCO (He et al., 2020) constructs a dynamic dictionary using a moving average encoder and queue, and minimizes contrastive loss with the dictionary. On the other hand, several non-contrastive works achieve remarkable performance. BYOL (Grill et al., 2020) encodes two different views of an input with a student and teacher encoder, respectively, and minimizes the distance between those two representations. Barlow Twins (Zbontar et al., 2021) constructs a correlation matrix between two different views of a batch of samples with an encoder and trains the encoder to enforce the correlation matrix to the identity matrix. Lastly, MAE (He et al., 2022) learns a meaningful image representation space by masking an image and reconstructing the masked input. In this paper, we utilize Barlow Twins as an SSL framework to train our target model.

3 METHOD

3.1 PRELIMINARIES

Problem Definition Suppose that we are given an unlabeled dataset $X_t = [\mathbf{x}_1 \cdots \mathbf{x}_n]^\top \in \mathbb{R}^{n \times d_x}$ where each row $\mathbf{x}_i \in \mathbb{R}^{d_x}$ is an i.i.d sample. We define the problem of *self-supervised dataset distillation* as the process of creating a compact synthetic dataset $X_s = [\hat{\mathbf{x}}_1 \cdots \hat{\mathbf{x}}_m]^\top \in \mathbb{R}^{m \times d_x}$ that preserves most of the information from the unlabeled dataset X_t for pre-training any neural networks, while keeping $m \ll n$. Thus, after the dataset distillation process, we can transfer knowledge embedded in the large dataset to various tasks using the distilled dataset. Specifically, our final goal is to accelerate the pre-training of a neural network with any architectures by utilizing the distilled dataset X_s in place of the full unlabeled dataset X_t for pre-training. Subsequently, one can evaluate the performance of the neural network by fine-tuning it on various downstream tasks.

Bilevel Optimization with SSL Recent success of transfer learning with self-supervised learning (SSL) (Chen et al., 2020a; He et al., 2020; Grill et al., 2020; Zbontar et al., 2021) is deeply rooted in the ability to learn meaningful and task-agnostic latent representation space. Inspired by the SSL, we want to find a distilled dataset X_s such that a model $\hat{g}_\theta : \mathbb{R}^{d_x} \rightarrow \mathbb{R}^{d_y}$, trained on X_s with a SSL objective, achieves low SSL loss on the full dataset X_t . Here, θ denotes the parameter of the neural network \hat{g}_θ . Similar to previous supervised dataset condensation methods (Wang et al., 2018; Zhao et al., 2021; Cazenavette et al., 2022; Deng & Russakovsky, 2022), estimation of X_s can be formulated as a bilevel optimization problem:

$$\underset{X_s}{\text{minimize}} \mathcal{L}_{\text{SSL}}(\theta^*(X_s); X_t), \text{ where } \theta^*(X_s) = \arg \min_{\theta} \mathcal{L}_{\text{SSL}}(\theta; X_s). \quad (1)$$

Here, $\mathcal{L}_{\text{SSL}}(\theta; X_s)$ denotes a SSL loss function with \hat{g}_θ evaluated on the dataset X_s . The bilevel optimization can be solved by iterative gradient-based algorithms. However, it is computationally expensive since computing gradient with respect to X_s requires back-propagating through unrolled computational graphs of inner optimization steps. Furthermore, we empirically find out that back-propagating through data augmentations involved in SSL is unstable and challenging.

3.2 KERNEL RIDGE REGRESSION ON SELF-SUPERVISED TARGET

Motivation We theoretically analyze the instability of the bilevel formulation for optimizing a condensed dataset with a SSL objective and motivate our objective function. Define d_θ by $\theta \in \mathbb{R}^{d_\theta}$. Let us write $\mathcal{L}_{\text{SSL}}(\theta; X_s) = \mathbb{E}_{\xi \sim \mathcal{D}}[\ell_\xi(\theta, X_s)]$ where $\xi \sim \mathcal{D}$ is the random variable corresponding to the data augmentation (or input mask), and ℓ_ξ is SSL loss with the sampled data augmentation (or input mask) ξ . Define $\hat{\theta}(X_s) = \arg \min_{\theta} \hat{\mathcal{L}}_{\text{SSL}}(\theta; X_s)$ where $\hat{\mathcal{L}}_{\text{SSL}}(\theta; X_s) = \frac{1}{r} \sum_{i=1}^r \ell_{\zeta_i}(\theta, X_s)$ and $\zeta_i \sim \mathcal{D}$. In practice, we compute $\frac{\partial \hat{\mathcal{L}}_{\text{SSL}}(\hat{\theta}(X_s); X_t)}{\partial X_s}$ to update X_s . The use of the empirical estimate $\hat{\mathcal{L}}_{\text{SSL}}(\theta; X_s)$ in the place of the true SSL loss $\mathcal{L}_{\text{SSL}}(\theta; X_s)$ is justified in standard SSL without bilevel optimization because its gradient is always an unbiased estimator of the true gradient: *i.e.*, $\mathbb{E}_\zeta[\frac{\partial \hat{\mathcal{L}}_{\text{SSL}}(\theta; X_s)}{\partial \theta}] = \frac{\partial \mathcal{L}_{\text{SSL}}(\theta; X_s)}{\partial \theta}$ where $\zeta = (\zeta_i)_{i=1}^r$. However, the following theorem shows that this is not the case for bilevel optimization. This explains the empirically observed instability of the SSL loss in bilevel optimization. A proof is deferred to Appendix A.

Theorem 1. *The derivative $\frac{\partial \mathcal{L}_{\text{SSL}}(\hat{\theta}(X_s); X_t)}{\partial X_s}$ is a biased estimator of $\frac{\partial \mathcal{L}_{\text{SSL}}(\theta^*(X_s); X_t)}{\partial X_s}$, i.e., $\mathbb{E}_\zeta[\frac{\partial \mathcal{L}_{\text{SSL}}(\hat{\theta}(X_s); X_t)}{\partial X_s}] \neq \frac{\partial \mathcal{L}_{\text{SSL}}(\theta^*(X_s); X_t)}{\partial X_s}$, unless $(\frac{\partial \mathcal{L}_{\text{SSL}}(\theta; X_t)}{\partial \theta}|_{\theta=\theta^*(X_s)}) \frac{\partial \theta^*(X_s)}{\partial (X_s)_{ij}} = \mathbb{E}_\zeta[\frac{\partial \mathcal{L}_{\text{SSL}}(\theta; X_t)}{\partial \theta}|_{\theta=\hat{\theta}(X_s)}] \mathbb{E}_\zeta[\frac{\partial \hat{\theta}(X_s)}{\partial (X_s)_{ij}}] + \sum_{k=1}^{d_\theta} \text{Cov}_\zeta[\frac{\partial \mathcal{L}_{\text{SSL}}(\theta; X_t)}{\partial \theta_k}|_{\theta=\hat{\theta}(X_s)}, \frac{\partial \hat{\theta}(X_s)_k}{\partial (X_s)_{ij}}]$ for all $(i, j) \in \{1, \dots, m\} \times \{1, \dots, d_x\}$.*

Regression on Self-supervised Target Based on the insight of Theorem 1, we propose to replace the inner objective function with a mean squared error (MSE) by parameterizing and optimizing both synthetic examples X_s and their target representations $Y_s = [\hat{y}_1 \cdots \hat{y}_m]^\top \in \mathbb{R}^{m \times d_y}$ as:

$$\mathcal{L}_{\text{inner}}(\theta; X_s, Y_s) = \frac{1}{2} \|Y_s - \hat{g}_\theta(X_s)\|_F^2, \quad (2)$$

which avoids the biased gradient of SSL loss due to the absence of random variables ζ corresponding to data augmentation (or input mask) in the MSE. Here, $\|\cdot\|_F$ denotes a Frobenius norm. Similarly, we replace the outer objective with the MSE between the original data representation of the model trained with $\mathcal{L}_{\text{inner}}(\theta; X_s, Y_s)$ and that of the target model $g_\phi : \mathbb{R}^{d_x} \rightarrow \mathbb{R}^{d_y}$ trained on the full dataset X_t with the SSL objective as follows:

$$\underset{X_s, Y_s}{\text{minimize}} \frac{1}{2} \|g_\phi(X_t) - \hat{g}_{\theta^*(X_s, Y_s)}(X_t)\|_F^2, \text{ where } \theta^*(X_s, Y_s) = \arg \min_{\theta} \mathcal{L}_{\text{inner}}(\theta; X_s, Y_s). \quad (3)$$

Note that we first pre-train the target model g_ϕ on the full dataset X_t with the SSL objective, *i.e.*, $\phi = \arg \min_{\phi} \mathcal{L}_{\text{SSL}}(\phi; X_t)$. After that, $g_\phi(X_t)$ is a fixed target which is considered to be constant during the optimization of X_s and Y_s . Here, $g_\phi(X_t) = [g_\phi(\mathbf{x}_1) \cdots g_\phi(\mathbf{x}_n)]^\top \in \mathbb{R}^{n \times d_y}$ and $\hat{g}_{\theta^*(X_s, Y_s)}(X_t) = [\hat{g}_{\theta^*(X_s, Y_s)}(\mathbf{x}_1) \cdots \hat{g}_{\theta^*(X_s, Y_s)}(\mathbf{x}_n)]^\top \in \mathbb{R}^{n \times d_y}$. The intuition behind the objective function is as follows. Assuming that a model trained with a SSL objective on a large-scale dataset generalizes to various downstream tasks (Chen et al., 2020b), we aim to ensure that the representation space of the model $\hat{g}_{\theta^*(X_s, Y_s)}$, trained on the condensed data, is similar to that of the self-supervised target model g_ϕ .

Algorithm 1 Kernel Ridge Regression on Self-supervised Target (KRR-ST)

```

1: Input: Dataset  $X_t$ , batch size  $b$ , learning rate  $\alpha, \eta$ , SSL objective  $\mathcal{L}_{\text{SSL}}$ , and total steps  $T$ .
2: Optimize  $g_\phi$  with SSL loss on  $X_t$ :  $\phi \leftarrow \arg \min_\phi \mathcal{L}_{\text{SSL}}(\phi; X_t)$ .
3: Initialize  $X_s = [\hat{\mathbf{x}}_1 \cdots \hat{\mathbf{x}}_m]^\top$  and  $Y_s = [\hat{\mathbf{y}}_1 \cdots \hat{\mathbf{y}}_m]^\top$ .
4: Initialize a model pool  $\mathcal{M} = \{(\omega_1, W_1, t_1), \dots, (\omega_l, W_l, t_l)\}$  using  $X_s$  and  $Y_s$ .
5: while not converged do
6:   Uniformly sample a mini batch  $\bar{X}_t = [\bar{\mathbf{x}}_1 \cdots \bar{\mathbf{x}}_b]^\top$  from the full dataset  $X_t$ .
7:   Uniformly sample an index  $i$  from  $\{1, \dots, l\}$  and retrieve the model  $(\omega_i, W_i, t_i) \in \mathcal{M}$ .
8:   Compute the outer objective  $\mathcal{L}_{\text{outer}}(X_s, Y_s)$  with  $f_{\omega_i}$  in equation 4.
9:   Update  $X_s$  and  $Y_s$ .  $X_s \leftarrow X_s - \alpha \nabla_{X_s} \mathcal{L}_{\text{outer}}(X_s, Y_s)$ ,  $Y_s \leftarrow Y_s - \alpha \nabla_{Y_s} \mathcal{L}_{\text{outer}}(X_s, Y_s)$ .
10:  if  $t_i < T$  then
11:    Set  $t_i \leftarrow t_i + 1$  and evaluate MSE loss  $\mathcal{L}_{\text{MSE}} \leftarrow \frac{1}{2} \|Y_s - h_{W_i} \circ f_{\omega_i}(X_s)\|_F^2$ .
12:    Update  $\omega_i$  and  $W_i$  with  $\omega_i \leftarrow \omega_i - \eta \nabla_{\omega_i} \mathcal{L}_{\text{MSE}}$ ,  $W_i \leftarrow W_i - \eta \nabla_{W_i} \mathcal{L}_{\text{MSE}}$ .
13:  else
14:    Set  $t_i \leftarrow 0$  and randomly initialize  $\omega_i$  and  $W_i$ .
15:  end if
16: end while
17: Output: Distilled dataset  $(X_s, Y_s)$ 

```

Again, one notable advantage of using the MSE is that it removes the need for data augmentations or masking inputs for the evaluation of the inner objective. Furthermore, we can easily evaluate the inner objective with full batch X_s since the size of X_s (*i.e.*, m) is small enough and we do not need $m \times m$ pairwise correlation matrix required for many SSL objectives (Chen et al., 2020a; He et al., 2020; Zbontar et al., 2021; Bardes et al., 2022). Consequently, the elimination of randomness enables us to get an unbiased estimate of the true gradient and contributes to stable optimization.

Kernel Ridge Regression Lastly, following Zhou et al. (2022), we simplify the inner optimization to reduce the computational cost of bilevel optimization in equation 3. First, we decompose the function \hat{g}_θ into a feature extractor $f_\omega : \mathbb{R}^{d_x} \rightarrow \mathbb{R}^{d_h}$ and a linear head $h_W : \mathbf{v} \in \mathbb{R}^{d_h} \mapsto \mathbf{v}^\top W \in \mathbb{R}^{d_y}$, where $W \in \mathbb{R}^{d_h \times d_y}$, and $\theta = (\omega, W)$ (*i.e.*, $\hat{g}_\theta = h_W \circ f_\omega$). Naively, we can train the feature extractor and linear head on X_s and Y_s during inner optimization and compute the meta-gradient of X_s and Y_s w.r.t. the outer objective while considering the feature extractor constant. However, previous works (Cazenavette et al., 2022; Zhou et al., 2022; Zhao et al., 2023) have shown that using diverse models at inner optimization is robust to overfitting compared to using a single model.

Based on this insight, we maintain a model pool \mathcal{M} consisting of l different feature extractors and linear heads. To initialize each $h_W \circ f_\omega$ in the pool, we first sample $t \in \{1, \dots, T\}$ and then optimize ω and W to minimize the MSE in equation 2 on randomly initialized X_s and Y_s with full-batch gradient descent algorithms for t steps, where T is the maximum number of steps. Afterward, we sample a feature extractor f_ω from \mathcal{M} for each meta-update. We then optimize another head h_{W^*} on top of the sampled feature extractor f_ω which is fixed. Here, kernel ridge regression (Murphy, 2012) enables getting a closed form solution of the linear head as $h_{W^*} : \mathbf{v} \mapsto \mathbf{v}^\top f_\omega(X_s)^\top (K_{X_s, X_s} + \lambda I_m)^{-1} Y_s$, where $\lambda > 0$ is a hyperparameter for ℓ_2 regularization, $I_m \in \mathbb{R}^{m \times m}$ is an identity matrix, and $K_{X_s, X_s} = f_\omega(X_s) f_\omega(X_s)^\top \in \mathbb{R}^{m \times m}$ with $f_\omega(X_s) = [f_\omega(\hat{\mathbf{x}}_1) \cdots f_\omega(\hat{\mathbf{x}}_m)]^\top \in \mathbb{R}^{m \times d_h}$. Then, we sample a mini-batch $\bar{X}_t = [\bar{\mathbf{x}}_1 \cdots \bar{\mathbf{x}}_b]^\top \in \mathbb{R}^{b \times d_x}$ from the full set X_t and compute a meta-gradient of X_s and Y_s with respect to the following outer objective function:

$$\mathcal{L}_{\text{outer}}(X_s, Y_s) = \frac{1}{2} \|g_\phi(\bar{X}_t) - f_\omega(\bar{X}_t) f_\omega(X_s)^\top (K_{X_s, X_s} + \lambda I_m)^{-1} Y_s\|_F^2, \quad (4)$$

where $g_\phi(\bar{X}_t) = [g_\phi(\bar{\mathbf{x}}_1) \cdots g_\phi(\bar{\mathbf{x}}_b)]^\top \in \mathbb{R}^{b \times d_y}$ and $f_\omega(\bar{X}_t) = [f_\omega(\bar{\mathbf{x}}_1) \cdots f_\omega(\bar{\mathbf{x}}_b)]^\top \in \mathbb{R}^{b \times d_h}$. Finally, we update the distilled dataset X_s and Y_s with gradient descent algorithms. After updating the distilled dataset, we update the selected feature extractor f_ω and its corresponding head h_W with the distilled dataset for one step. Based on this, we dub our proposed method as **Kernel Ridge Regression on Self-supervised Target (KRR-ST)**, and outline its algorithmic design in Algorithm 1.

Transfer Learning We now elaborate on how we deploy the distilled dataset for transfer learning scenarios. Given the distilled dataset (X_s, Y_s) , we first pre-train a randomly initialized feature extractor f_ω and head $h_W : \mathbf{v} \in \mathbb{R}^{d_h} \mapsto \mathbf{v}^\top W \in \mathbb{R}^{d_y}$ on the distilled dataset to minimize either MSE for our KRR-ST, KIP (Nguyen et al., 2021a), and FRePO (Zhou et al., 2022), or cross-entropy

loss for DSA (Zhao & Bilen, 2021), MTT (Cazenavette et al., 2022), and DM (Zhao & Bilen, 2023):

$$\underset{\omega, W}{\text{minimize}} \frac{1}{2} \|f_\omega(X_s)W - Y_s\|_F^2, \quad \text{or} \quad \underset{\omega, W}{\text{minimize}} \sum_{i=1}^m \ell(\hat{y}_i, \text{softmax}(f_\omega(\hat{x}_i)^\top W)), \quad (5)$$

where $\ell(\mathbf{p}, \mathbf{q}) = -\sum_{i=1}^c p_i \log q_i$ for $\mathbf{p} = (p_1, \dots, p_c), \mathbf{q} = (q_1, \dots, q_c) \in \Delta^{c-1}$, and Δ^{c-1} is simplex over \mathbb{R}^c . Then, we discard h_W and fine-tune the feature extractor f_ω with a randomly initialized task-specific head $h_Q : \mathbf{v} \in \mathbb{R}^{d_h} \mapsto \text{softmax}(\mathbf{v}^\top Q) \in \Delta^{c-1}$ on a target labeled dataset to minimize the cross-entropy loss ℓ . Here, $Q \in \mathbb{R}^{d_h \times c}$ and c is the number of classes. Note that we can use any loss function for fine-tuning, however, we only focus on the classification in this work.

4 EXPERIMENTS

In this section, we empirically validate the efficacy of our KKR-ST on various applications: transfer learning, architecture generalization, and target data-free knowledge distillation.

4.1 EXPERIMENTAL SETUPS

Datasets We use either CIFAR100 (Krizhevsky et al., 2009), TinyImageNet (Le & Yang, 2015), or ImageNet (Deng et al., 2009) as a source dataset for dataset distillation, while evaluating the distilled dataset on CIFAR10 (Krizhevsky et al., 2009), Aircraft (Maji et al., 2013), Stanford Cars (Krause et al., 2013), CUB2011 (Wah et al., 2011), Stanford Dogs (Khosla et al., 2011), and Flowers (Nilsback & Zisserman, 2008). For ImageNet, we resize the images into a resolution of 64×64 , following the previous dataset distillation methods (Zhou et al., 2022; Cazenavette et al., 2022). We resize the images of the target dataset into the resolution of the source dataset, e.g., 32×32 for CIFAR100 and 64×64 for TinyImageNet and ImageNet, respectively.

Baselines We compare the proposed method KRR-ST with 8 different baselines including a simple baseline without pre-training, 5 representative baselines from the dataset condensation benchmark (Cui et al., 2022), and 2 kernel ridge regression baselines as follows:

- 1) **w/o pre**: We train a model on solely the target dataset without any pre-training.
- 2) **Random**: We pre-train a model on randomly chosen images of the source dataset.
- 3) **Kmeans** (Cui et al., 2022): Instead of 2) **Random** choice, we choose the nearest image for each centroid of kmeans-clustering (Lloyd, 1982) in feature space of the source dataset.
- 4-6) **DSA** (Zhao & Bilen, 2021), **DM** (Zhao & Bilen, 2023), and **MTT** (Cazenavette et al., 2022): These are representative dataset condensation methods based on surrogate objectives such as gradient matching, distribution matching, and trajectory matching, respectively.
- 7) **KIP** (Nguyen et al., 2021a;b): Kernel Inducing Points (KIP) is the first proposed kernel ridge regression method for dataset distillation. For transfer learning, we use the distilled datasets with standard normalization instead of ZCA-whitening.
- 8) **FRePo** (Zhou et al., 2022): Feature Regression with Pooling (FRePo) is a relaxed version of bilevel optimization, where inner optimization is replaced with the analytic solution of kernel ridge regression on neural features. Since FRePo does not provide datasets distilled with standard normalization, we use ZCA-whitening obtained from a source dataset for normalization.

Implementation Details Following Nguyen et al. (2021a;b); Zhou et al. (2022), we use convolutional layers consisting of batch normalization (Ioffe & Szegedy, 2015), ReLU activation, and average pooling for distilling a dataset. We choose the number of layers based on the resolution of images, *i.e.*, 3 layers for 32×32 and 4 layers for 64×64 , respectively. We initialize and maintain $l = 10$ models for the model pool \mathcal{M} , and update the models in the pool using full-batch gradient descent with learning rate, momentum, and weight decay being set to 0.1, 0.9, and 0.001, respectively. The total number of steps T is set to 1,000. We meta-update our distilled dataset for 160,000 iterations using AdamW optimizer (Loshchilov & Hutter, 2019) with an initial learning rate of 0.001 and the learning rate is linearly decayed. We use ResNet18 (He et al., 2016) as a self-supervised target model g_ϕ which is trained on a source dataset with Barlow Twins (Zbontar et al., 2021) objective.

After distillation, we pre-train a model on the distilled dataset for 1,000 epochs with a mini-batch size of 256 using stochastic gradient descent (SGD) optimizer, where learning rate and momentum are set to 0.1 and 0.9, respectively. The weight decay is set to 0.001 for CIFAR100 and ImageNet, and 0.0005 for TinyImageNet. For the baselines, we follow their original experimental setup to pre-train a model on their condensed dataset. For fine-tuning, all the experimental setups are fixed as follows: we use the SGD optimizer with momentum of 0.9 and without weight decay, where the learning rate of a feature extractor and task-specific head are set to 0.005 and 0.05, respectively. The learning rate is decayed with cosine scheduling. Note that we did not extensively search hyperparameters for fine-tuning each architecture and one can improve the reported performance by tuning the hyperparameters. Our code is included in the Supplementary File.

4.2 EXPERIMENTAL RESULTS AND ANALYSIS

Table 1: The results of **transfer learning with CIFAR100**. The data compression ratio for source dataset is 2%. ConvNet3 is pre-trained on condensed dataset, and then fine-tuned on target datasets. We report the average and standard deviation over three runs. The best results are bolded.

Method	Source	Target					
		CIFAR100	CIFAR10	Aircraft	Cars	CUB2011	Dogs
w/o pre	62.53 \pm 0.15	85.95 \pm 0.13	18.15 \pm 0.57	11.59 \pm 0.70	14.41 \pm 0.70	18.00 \pm 0.27	32.61 \pm 0.73
Random	62.40 \pm 0.11	83.32 \pm 0.37	17.13 \pm 2.25	15.17 \pm 0.19	15.37 \pm 0.41	19.11 \pm 0.16	53.10 \pm 0.37
Kmeans	62.59 \pm 0.27	83.23 \pm 0.52	19.62 \pm 1.49	15.45 \pm 0.19	15.49 \pm 0.18	19.01 \pm 0.25	57.88 \pm 0.32
DSA	62.45 \pm 0.32	83.57 \pm 0.36	18.03 \pm 0.81	15.06 \pm 0.21	15.11 \pm 0.02	18.73 \pm 0.07	57.72 \pm 0.31
DM	62.71 \pm 0.09	83.42 \pm 0.16	18.78 \pm 1.18	15.77 \pm 0.18	16.30 \pm 0.09	19.23 \pm 0.36	57.88 \pm 0.21
MTT	63.52 \pm 0.36	83.52 \pm 0.40	17.00 \pm 2.39	16.53 \pm 0.21	16.52 \pm 0.43	20.03 \pm 0.40	60.64 \pm 0.35
KIP	63.78 \pm 0.18	85.04 \pm 0.46	21.53 \pm 2.37	18.03 \pm 0.22	18.30 \pm 0.06	21.30 \pm 0.03	56.98 \pm 0.24
FRePo	64.49 \pm 0.21	86.69 \pm 0.13	24.40 \pm 0.72	19.65 \pm 0.67	21.83 \pm 0.04	23.33 \pm 0.13	56.16 \pm 0.11
KRR-ST	66.46 \pm 0.12	88.87 \pm 0.05	32.94 \pm 0.21	23.92 \pm 0.09	24.38 \pm 0.18	23.39 \pm 0.24	64.28 \pm 0.16

Table 2: The results of **transfer learning with TinyImageNet**. The data compression ratio for source dataset is 2%. ConvNet4 is pre-trained on condensed dataset, and then fine-tuned on target datasets. We report the average and standard deviation over three runs. The best results are bolded.

Method	Source	Target					
		TinyImageNet	CIFAR10	Aircraft	Cars	CUB2011	Dogs
w/o pre	50.18 \pm 0.32	87.54 \pm 0.18	28.54 \pm 0.56	18.16 \pm 0.39	18.16 \pm 0.90	11.35 \pm 0.06	49.28 \pm 0.54
Random	45.62 \pm 0.14	83.92 \pm 0.79	21.23 \pm 4.87	18.89 \pm 0.28	17.55 \pm 0.27	20.68 \pm 0.53	57.21 \pm 0.27
Kmeans	46.02 \pm 0.53	82.88 \pm 0.93	23.34 \pm 3.08	20.24 \pm 0.35	18.40 \pm 0.20	21.47 \pm 0.31	57.89 \pm 0.32
DSA	46.38 \pm 0.54	84.58 \pm 0.40	19.62 \pm 6.42	19.90 \pm 0.39	18.61 \pm 0.20	21.79 \pm 0.25	57.72 \pm 0.31
DM	45.41 \pm 0.16	84.70 \pm 0.17	27.18 \pm 1.79	19.22 \pm 0.22	17.65 \pm 0.33	21.22 \pm 0.10	57.88 \pm 0.21
MTT	48.16 \pm 0.13	85.07 \pm 0.79	25.02 \pm 3.57	22.61 \pm 0.10	21.02 \pm 0.19	24.44 \pm 0.33	60.64 \pm 0.35
FRePo	46.40 \pm 0.50	87.55 \pm 0.10	38.52 \pm 1.88	24.86 \pm 2.75	25.78 \pm 0.76	27.51 \pm 0.74	60.46 \pm 2.13
KRR-ST	51.57 \pm 0.09	89.28 \pm 0.16	47.08 \pm 1.11	47.76 \pm 0.49	32.84 \pm 0.52	35.12 \pm 0.21	66.28 \pm 0.44

Table 3: The results of **transfer learning with ImageNet**. The data compression ratio for the source dataset is \approx 0.08%. ConvNet4 is pre-trained on condensed datasets and then fine-tuned on target datasets. We report the average and standard deviation over three runs. The best results are bolded.

Method	CIFAR10	CIFAR100	Aircraft	Cars	CUB2011	Dogs	Flowers
w/o pre	87.54 \pm 0.18	64.54 \pm 0.07	28.54 \pm 0.56	18.16 \pm 0.39	18.16 \pm 0.90	11.35 \pm 0.06	49.28 \pm 0.54
Random	84.09 \pm 0.50	61.60 \pm 0.21	19.28 \pm 1.15	15.86 \pm 0.10	15.59 \pm 0.21	18.48 \pm 0.35	51.02 \pm 0.29
FRePo	86.98 \pm 0.12	63.45 \pm 0.43	7.84 \pm 1.07	12.74 \pm 2.47	16.97 \pm 1.72	23.20 \pm 0.16	30.26 \pm 6.88
KRR-ST	89.00 \pm 0.15	67.62 \pm 0.21	43.39 \pm 1.21	37.38 \pm 0.80	31.65 \pm 0.24	33.99 \pm 0.26	64.88 \pm 0.62

Transfer learning We investigate how our proposed KRR-ST can be effectively used for transfer learning. To this end, we pre-train a model on the distilled source dataset and fine-tune the model using a target training dataset. We report the average and standard deviation of the model’s accuracy on the target test dataset over three runs. First, we use ConvNet3 (3-layer CNN) to distill the CIFAR100 dataset into 1,000 synthetic examples, which is equivalent to 2% of the original dataset.

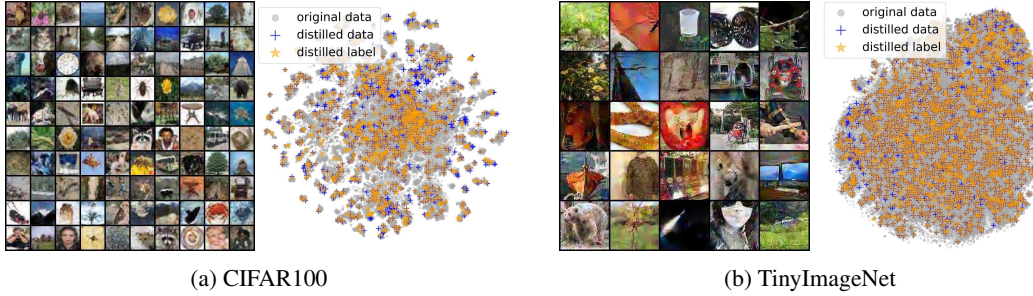


Figure 2: **Visualization** of the distilled images, their feature representation and corresponding distilled labels in the output space of the target model. All distilled images are provided in Appendix B.

Table 4: The results of **architecture generalization**. ConvNet4 is utilized for condensing TinyImageNet into 2,000 synthetic examples. Models with different architectures are pre-trained on the condensed dataset and fine-tuned on target datasets. We report the average and standard deviation over three runs.

Method	Cars				Dogs			
	VGG11	AlexNet	MobileNet	ResNet10	VGG11	AlexNet	MobileNet	ResNet10
w/o pre	24.90 \pm 0.67	18.38 \pm 0.12	3.94 \pm 0.34	2.43 \pm 0.08	27.33 \pm 0.39	21.91 \pm 0.12	9.28 \pm 0.17	3.03 \pm 0.16
Random	26.80 \pm 0.70	19.79 \pm 0.20	16.12 \pm 1.16	8.76 \pm 0.22	27.58 \pm 0.43	17.51 \pm 1.81	20.44 \pm 0.75	16.05 \pm 0.46
Kmeans	28.13 \pm 0.06	20.47 \pm 0.31	19.31 \pm 1.25	9.62 \pm 0.17	28.28 \pm 0.35	19.03 \pm 1.80	22.37 \pm 0.72	17.18 \pm 0.25
DSA	26.83 \pm 0.50	20.43 \pm 0.40	16.68 \pm 1.12	9.14 \pm 0.44	27.74 \pm 0.51	21.06 \pm 0.95	21.34 \pm 0.90	17.24 \pm 0.41
DM	26.74 \pm 0.21	18.76 \pm 0.30	19.94 \pm 0.70	9.46 \pm 0.46	28.34 \pm 0.08	20.36 \pm 0.17	23.03 \pm 0.49	17.56 \pm 0.23
MTT	34.80 \pm 0.28	24.45 \pm 0.47	21.71 \pm 0.07	10.80 \pm 0.28	32.41 \pm 0.55	23.81 \pm 0.46	27.04 \pm 0.44	19.49 \pm 0.61
FRePo	31.37 \pm 0.42	28.33 \pm 0.81	15.51 \pm 0.34	2.23 \pm 0.24	29.86 \pm 0.72	24.66 \pm 0.69	22.75 \pm 0.57	6.63 \pm 0.27
KRR-ST	52.78\pm0.93	38.20\pm1.26	38.81\pm0.94	21.41\pm1.31	39.10\pm0.12	30.49\pm0.46	39.10\pm0.28	31.83\pm0.86

After distillation, we pre-train the model with the synthetic samples and fine-tune it on the target training datasets. As shown in Table 1, KRR-ST outperforms all the baselines, including those using labels for distillation, except for the Standford Dogs dataset. Next, we distill TinyImageNet into 2,000 synthetic images, which constitute 2% of the original dataset. We pre-train ConvNet4 on the distilled dataset and fine-tune the model on the target datasets. As shown in Table 2, we observe that our unsupervised dataset distillation method outperforms all the baselines by a larger margin than in the previous experiments with the distilled CIFAR100 dataset.

Lastly, we distill ImageNet into 1,000 synthetic samples which are approximately 0.08% of the original full dataset using ConvNet4, and report experimental results in Table 3. For ImageNet experiments, FRePo is the only available supervised dataset distillation method since we can not run the other baselines due to their large memory consumption. Furthermore, we present better accuracy for FRePo, achieved through either ZCA-whitening on target data or reverse ZCA-whitening on distilled data. This is because the ZCA-whitening of ImageNet does not work effectively with certain datasets. As in the previous experiments, our method consistently outperforms all the baselines across target datasets. These experimental results demonstrate the efficacy of our method in condensing an unlabeled dataset for pre-training a model that can be transferred to target datasets.

Visualization In this paragraph, we analyze how our method distills images and their corresponding target representations in both pixel and feature space. We first present the distilled images X_s and visualize their representation $g_\phi(X_s) \in \mathbb{R}^{512}$ along with the learned target representation $Y_s \in \mathbb{R}^{512}$ and representations of the original full data $g_\phi(X_t) \in \mathbb{R}^{512}$, where g_ϕ is the target ResNet18 trained with SSL Barlow Twins objective on the original dataset X_t . For visualization, we employ t-SNE (Van der Maaten & Hinton, 2008) to project the high-dimensional representations to 2D vectors. Figure 2 demonstrates the distilled images and corresponding feature space of CIFAR100 and TinyImageNet. As reported in Zhou et al. (2022), we have found that distilled images with our algorithm result in visually realistic samples, which is well-known to be a crucial factor for architecture generalization. Lastly, we observe that the distilled data points cover most of the feature space induced by the full dataset, even with either 1,000 or 2,000 synthetic samples which are only 2% of the full dataset. All distilled images are provided in Appendix B.

Architecture Generalization To examine whether our method can produce a distilled dataset that can be generalized to different architectures, we perform the following experiments. First, we use ConvNet4 as \hat{g}_θ in equation 3 to condense TinyImageNet into 2,000 synthetic examples. Then, we

Table 5: The results of **target data-free KD** on CIFAR10. ConvNet4 is utilized for condensing TinyImageNet into 2,000 synthetic examples. Models with different architectures are pre-trained on the condensed dataset and fine-tuned on CIFAR10 using KD loss. We report the average and standard deviation over three runs.

Method	ConvNet4	VGG11	AlexNet	MobileNet	ResNet10
Gaussian	32.45 \pm 0.65	33.25 \pm 1.33	30.58 \pm 0.56	23.96 \pm 0.94	24.83 \pm 1.86
Random	49.34 \pm 1.00	51.82 \pm 0.43	48.95 \pm 0.59	44.48 \pm 0.04	39.51 \pm 0.52
Kmeans	52.37 \pm 0.35	53.92 \pm 0.20	51.33 \pm 0.60	46.87 \pm 0.40	41.96 \pm 0.31
DSA	45.17 \pm 0.79	47.68 \pm 0.53	44.58 \pm 0.83	39.89 \pm 1.11	37.88 \pm 0.46
DM	45.15 \pm 0.69	47.64 \pm 0.65	45.31 \pm 0.35	41.07 \pm 0.86	38.81 \pm 0.29
MTT	49.12 \pm 0.68	53.89 \pm 0.69	48.92 \pm 0.63	43.63 \pm 0.74	38.70 \pm 0.92
FRePO	46.26 \pm 0.52	49.40 \pm 0.26	41.32 \pm 2.30	41.18 \pm 0.07	43.41 \pm 0.81
KRR-ST	59.04\pm0.45	63.40\pm0.54	59.21\pm0.31	55.09\pm0.28	53.75\pm1.11

pre-train models of VGG11 (Simonyan & Zisserman, 2015), AlexNet (Krizhevsky et al., 2012), MobileNet (Howard et al., 2017), and ResNet10 (Gong et al., 2022) architectures on the condensed dataset. Finally, the models are fine-tuned on five target datasets — Stanford Cars, Stanford Dogs, Aircraft, CUB2011, and Flowers dataset. We choose those architectures since they are lightweight and suitable for small devices, and pre-trained weights of those architectures for 64×64 resolution are rarely available on the internet. As shown in Table 4 and Tables 6 to 9 from Appendix C, our method achieves significant improvements over baselines across different architectures except for two settings (MobileNet on Aircraft and ResNet10 on Flowers). These results showcase that our method can effectively distill the source dataset into a small one that allows pre-training models with different architectures.

Target Data-Free Knowledge Distillation One of the most challenging transfer learning scenarios is data-free knowledge distillation (KD) (Lopes et al., 2017; Yin et al., 2020; Raikwar & Mishra, 2022), where we aim to distill the knowledge of teacher into smaller student models without a target dataset due to data privacy or intellectual property issues. Inspired by the success of KD with a surrogate dataset (Orekondy et al., 2019; Kim et al., 2023), we utilize distilled TinyImageNet dataset X_s as a surrogate dataset for KD instead of using the target dataset CIFAR10. Here, we investigate the efficacy of each dataset distillation method on this target data-free KD task. First, we are given a teacher model $T_\psi : \mathbb{R}^{d_x} \rightarrow \Delta^{c-1}$ which is trained on the target dataset CIFAR10, where $c = 10$ is the number of classes. We first pre-train a feature extractor f_ω , as demonstrated in equation 5. After that, we randomly initialize the task head $h_Q : \mathbf{v} \in \mathbb{R}^{d_h} \mapsto \text{softmax}(\mathbf{v}^\top Q) \in \Delta^{c-1}$ with $Q \in \mathbb{R}^{d_h \times c}$, and fine-tune ω and Q with the cross-entropy loss ℓ using the teacher T_ψ as a target:

$$\underset{\omega, Q}{\text{minimize}} \frac{1}{m} \sum_{i=1}^m \ell(T_\psi(\hat{\mathbf{x}}_i), \text{softmax}(f(\hat{\mathbf{x}}_i)^\top Q)). \quad (6)$$

In preliminary experiments, we have found that direct use of distilled dataset X_s for KD is not beneficial due to the discrepancy between the source and target dataset. To address this issue, we always use a mean and standard deviation of current mini-batch for batch normalization in both student and teacher models, even at test time, as suggested in Raikwar & Mishra (2022). We optimize the parameter ω and Q of the student model for 1,000 epochs with a mini-batch size of 512, using an AdamW optimizer with a learning rate of 0.001. Besides the supervised dataset distillation baselines, we introduce another baseline (Raikwar & Mishra, 2022) referred to as ‘‘Gaussian’’, which uses Gaussian noise as an input to the teacher and the student for computing the KD loss in equation 6, *i.e.*, $\hat{\mathbf{x}}_i \sim \mathcal{N}(\mathbf{0}, I_{d_x})$. Table 5 presents the results of target data-free KD experiments on CIFAR10. Firstly, we observe that utilizing a condensed surrogate dataset is more effective for knowledge distillation than using a Gaussian noise. Moreover, supervised dataset distillation methods (DSA, DM, and MTT) even perform worse than the baseline Random. On the other hand, our proposed KRR-ST consistently outperforms all the baselines across different architectures, which showcases the effectiveness of our method for target data-free KD.

5 CONCLUSION

In this work, we proposed a novel problem of unsupervised dataset distillation where we distill an unlabeled dataset into a small set of synthetic samples on which we pre-train a model on, and

fine-tune the model on the target datasets. Based on a theoretical analysis that the gradient of the synthetic samples with respect to existing SSL loss in naive bilevel optimization is biased, we proposed minimizing the mean squared error (MSE) between a model’s representation of the synthetic samples and learnable target representations for the inner objective. Based on the motivation that the model obtained by the inner optimization is expected to imitate the self-supervised target model, we also introduced the MSE between representations of the inner model and those of the self-supervised target model on the original full dataset for outer optimization. Finally, we simplify the inner optimization by optimizing only a linear head with kernel ridge regression, enabling us to reduce the computational cost. The experimental results demonstrated the efficacy of our self-supervised data distillation method in various applications such as transfer learning, architecture generalization, and target data-free knowledge distillation.

Reproducibility Statement We use Pytorch (Paszke et al., 2019) to implement our self-supervised dataset distillation method, KTT-RT. First, we have provided the complete proof of Theorem 1 in Appendix A. Moreover, we have detailed our method in Algorithm 1 and specified all the implementation details including hyperparameters in Section 4.1. Lastly, we have submitted our code in the Supplementary File.

Ethics Statement Our work is less likely to bring about any negative societal impacts. However, we should be careful about bias in the original dataset, as this bias may be transferred to the distilled dataset. On the positive side, we can significantly reduce the search cost of NAS, which, in turn, can reduce the energy consumption when running GPUs.

REFERENCES

Adrien Bardes, Jean Ponce, and Yann LeCun. VICReg: Variance-invariance-covariance regularization for self-supervised learning. In *International Conference on Learning Representations*, 2022.

Zalán Borsos, Mojmir Mutny, and Andreas Krause. Coresets via bilevel optimization for continual learning and streaming. *Advances in neural information processing systems*, 33:14879–14890, 2020.

George Cazenavette, Tongzhou Wang, Antonio Torralba, Alexei A Efros, and Jun-Yan Zhu. Dataset distillation by matching training trajectories. In *Proceedings of the IEEE/CVF Conference on Computer Vision and Pattern Recognition*, pp. 4750–4759, 2022.

Ting Chen, Simon Kornblith, Mohammad Norouzi, and Geoffrey Hinton. A simple framework for contrastive learning of visual representations. In *International conference on machine learning*, pp. 1597–1607. PMLR, 2020a.

Ting Chen, Simon Kornblith, Kevin Swersky, Mohammad Norouzi, and Geoffrey E Hinton. Big self-supervised models are strong semi-supervised learners. *Advances in neural information processing systems*, 33:22243–22255, 2020b.

Justin Cui, Ruochen Wang, Si Si, and Cho-Jui Hsieh. Dc-bench: Dataset condensation benchmark. *Advances in Neural Information Processing Systems*, 35:810–822, 2022.

Jia Deng, Wei Dong, Richard Socher, Li-Jia Li, Kai Li, and Fei-Fei Li. Imagenet: A large-scale hierarchical image database. In *2009 IEEE Computer Society Conference on Computer Vision and Pattern Recognition (CVPR 2009), 20-25 June 2009, Miami, Florida, USA*, pp. 248–255. IEEE Computer Society, 2009.

Zhiwei Deng and Olga Russakovsky. Remember the past: Distilling datasets into addressable memories for neural networks. In *Advances in Neural Information Processing Systems*, 2022.

Luca Franceschi, Michele Donini, Paolo Frasconi, and Massimiliano Pontil. Forward and reverse gradient-based hyperparameter optimization. In *International Conference on Machine Learning*, pp. 1165–1173. PMLR, 2017.

Jiaming Gong, Wei Liu, Mengjie Pei, Chengchao Wu, and Liufei Guo. Resnet10: A lightweight residual network for remote sensing image classification. In *International Conference on Measuring Technology and Mechatronics Automation (ICMTMA)*, pp. 975–978, 2022.

Jean-Bastien Grill, Florian Strub, Florent Altché, Corentin Tallec, Pierre Richemond, Elena Buchatskaya, Carl Doersch, Bernardo Avila Pires, Zhaohan Guo, Mohammad Gheshlaghi Azar, et al. Bootstrap your own latent-a new approach to self-supervised learning. *Advances in neural information processing systems*, 33:21271–21284, 2020.

Kaiming He, Xiangyu Zhang, Shaoqing Ren, and Jian Sun. Deep residual learning for image recognition. In *Proceedings of the IEEE conference on computer vision and pattern recognition*, pp. 770–778, 2016.

Kaiming He, Haoqi Fan, Yuxin Wu, Saining Xie, and Ross Girshick. Momentum contrast for unsupervised visual representation learning. In *Proceedings of the IEEE/CVF conference on computer vision and pattern recognition*, pp. 9729–9738, 2020.

Kaiming He, Xinlei Chen, Saining Xie, Yanghao Li, Piotr Dollár, and Ross Girshick. Masked autoencoders are scalable vision learners. In *Proceedings of the IEEE/CVF Conference on Computer Vision and Pattern Recognition*, pp. 16000–16009, 2022.

Andrew G Howard, Menglong Zhu, Bo Chen, Dmitry Kalenichenko, Weijun Wang, Tobias Weyand, Marco Andreetto, and Hartwig Adam. Mobilenets: Efficient convolutional neural networks for mobile vision applications. *arXiv preprint arXiv:1704.04861*, 2017.

Sergey Ioffe and Christian Szegedy. Batch normalization: Accelerating deep network training by reducing internal covariate shift. In *International conference on machine learning*, pp. 448–456. pmlr, 2015.

Aditya Khosla, Nityananda Jayadevaprakash, Bangpeng Yao, and Li Fei-Fei. Novel dataset for fine-grained image categorization. In *First Workshop on Fine-Grained Visual Categorization, IEEE Conference on Computer Vision and Pattern Recognition*, Colorado Springs, CO, June 2011.

Byungjoo Kim, Suyoung Lee, Seanie Lee, Sooel Son, and Sung Ju Hwang. Margin-based neural network watermarking. In *International Conference on Machine Learning*, 2023.

Jonathan Krause, Michael Stark, Jia Deng, and Li Fei-Fei. 3d object representations for fine-grained categorization. In *4th International IEEE Workshop on 3D Representation and Recognition (3dRR-13)*, Sydney, Australia, 2013.

Alex Krizhevsky, Geoffrey Hinton, et al. Learning multiple layers of features from tiny images, 2009.

Alex Krizhevsky, Ilya Sutskever, and Geoffrey E Hinton. Imagenet classification with deep convolutional neural networks. *Advances in neural information processing systems*, 25, 2012.

Ya Le and Xuan Yang. Tiny imagenet visual recognition challenge. *CS 231N*, 7(7):3, 2015.

Hayeon Lee, Sewoong Lee, Song Chong, and Sung Ju Hwang. Hardware-adaptive efficient latency prediction for NAS via meta-learning. In *Advances in Neural Information Processing Systems*, 2021.

Jaehoon Lee, Lechao Xiao, Samuel Schoenholz, Yasaman Bahri, Roman Novak, Jascha Sohl-Dickstein, and Jeffrey Pennington. Wide neural networks of any depth evolve as linear models under gradient descent. *Advances in neural information processing systems*, 32, 2019.

Hanxiao Liu, Karen Simonyan, and Yiming Yang. DARTS: Differentiable architecture search. In *International Conference on Learning Representations*, 2019.

Stuart Lloyd. Least squares quantization in pcm. *IEEE transactions on information theory*, 28(2): 129–137, 1982.

Noel Loo, Ramin Hasani, Alexander Amini, and Daniela Rus. Efficient dataset distillation using random feature approximation. *Advances in Neural Information Processing Systems*, 35:13877–13891, 2022.

Noel Loo, Ramin Hasani, Mathias Lechner, and Daniela Rus. Dataset distillation with convexified implicit gradients. *arXiv preprint arXiv:2302.06755*, 2023.

Raphael Gontijo Lopes, Stefano Fenu, and Thad Starner. Data-free knowledge distillation for deep neural networks. *arXiv preprint arXiv:1710.07535*, 2017.

David Lopez-Paz and Marc'Aurelio Ranzato. Gradient episodic memory for continual learning. *Advances in neural information processing systems*, 30, 2017.

Ilya Loshchilov and Frank Hutter. Decoupled weight decay regularization. In *International Conference on Learning Representations*, 2019.

Subhransu Maji, Esa Rahtu, Juho Kannala, Matthew Blaschko, and Andrea Vedaldi. Fine-grained visual classification of aircraft. *arXiv preprint arXiv:1306.5151*, 2013.

Baharan Mirzasoleiman, Jeff Bilmes, and Jure Leskovec. Coresets for data-efficient training of machine learning models. In *International Conference on Machine Learning*, pp. 6950–6960. PMLR, 2020.

Kevin P Murphy. *Machine learning: a probabilistic perspective*. MIT press, 2012.

Timothy Nguyen, Zhourong Chen, and Jaehoon Lee. Dataset meta-learning from kernel ridge-regression. In *International Conference on Learning Representations*, 2021a.

Timothy Nguyen, Roman Novak, Lechao Xiao, and Jaehoon Lee. Dataset distillation with infinitely wide convolutional networks. *Advances in Neural Information Processing Systems*, 34:5186–5198, 2021b.

Maria-Elena Nilsback and Andrew Zisserman. Automated flower classification over a large number of classes. In *2008 Sixth Indian conference on computer vision, graphics & image processing*, pp. 722–729. IEEE, 2008.

Tribhuvanesh Orekondy, Bernt Schiele, and Mario Fritz. Knockoff nets: Stealing functionality of black-box models. In *Proceedings of the IEEE/CVF conference on computer vision and pattern recognition*, pp. 4954–4963, 2019.

Adam Paszke, Sam Gross, Francisco Massa, Adam Lerer, James Bradbury, Gregory Chanan, Trevor Killeen, Zeming Lin, Natalia Gimelshein, Luca Antiga, et al. Pytorch: An imperative style, high-performance deep learning library. *Advances in neural information processing systems*, 32, 2019.

Piyush Raikwar and Deepak Mishra. Discovering and overcoming limitations of noise-engineered data-free knowledge distillation. *Advances in Neural Information Processing Systems*, 35:4902–4912, 2022.

Karen Simonyan and Andrew Zisserman. Very deep convolutional networks for large-scale image recognition. In *International Conference on Learning Representations, ICLR 2015*, 2015.

Laurens Van der Maaten and Geoffrey Hinton. Visualizing data using t-sne. *Journal of machine learning research*, 9(11), 2008.

C. Wah, S. Branson, P. Welinder, P. Perona, and S. Belongie. The caltech-ucsd birds-200-2011 dataset. Technical Report CNS-TR-2011-001, California Institute of Technology, 2011.

Tongzhou Wang, Jun-Yan Zhu, Antonio Torralba, and Alexei A Efros. Dataset distillation. *arXiv preprint arXiv:1811.10959*, 2018.

Hongxu Yin, Pavlo Molchanov, Jose M Alvarez, Zhizhong Li, Arun Mallya, Derek Hoiem, Niranjan K Jha, and Jan Kautz. Dreaming to distill: Data-free knowledge transfer via deepinversion. In *Proceedings of the IEEE/CVF Conference on Computer Vision and Pattern Recognition*, pp. 8715–8724, 2020.

Jure Zbontar, Li Jing, Ishan Misra, Yann LeCun, and Stéphane Deny. Barlow twins: Self-supervised learning via redundancy reduction. In *International Conference on Machine Learning*, pp. 12310–12320. PMLR, 2021.

Bo Zhao and Hakan Bilen. Dataset condensation with differentiable siamese augmentation. In *International Conference on Machine Learning*, 2021.

Bo Zhao and Hakan Bilen. Dataset condensation with distribution matching. In *Proceedings of the IEEE/CVF Winter Conference on Applications of Computer Vision*, pp. 6514–6523, 2023.

Bo Zhao, Konda Reddy Mopuri, and Hakan Bilen. Dataset condensation with gradient matching. In *International Conference on Learning Representations*, 2021.

Ganlong Zhao, Guanbin Li, Yipeng Qin, and Yizhou Yu. Improved distribution matching for dataset condensation. In *Proceedings of the IEEE/CVF Conference on Computer Vision and Pattern Recognition*, pp. 7856–7865, 2023.

Yongchao Zhou, Ehsan Nezhadarya, and Jimmy Ba. Dataset distillation using neural feature regression. *Advances in Neural Information Processing Systems*, 35:9813–9827, 2022.

A PROOF OF THEOREM 1

Proof. Let $(i,j) \in \{1, \dots, m\} \times \{1, \dots, d_x\}$. By the chain rule,

$$\frac{\partial \mathcal{L}_{\text{SSL}}(\theta^*(X_s); X_t)}{\partial (X_s)_{ij}} = \left(\frac{\partial \mathcal{L}_{\text{SSL}}(\theta; X_t)}{\partial \theta} \Big|_{\theta=\theta^*(X_s)} \right) \frac{\partial \theta^*(X_s)}{\partial (X_s)_{ij}} \quad (7)$$

Similarly,

$$\frac{\partial \mathcal{L}_{\text{SSL}}(\hat{\theta}(X_s); X_t)}{\partial (X_s)_{ij}} = \left(\frac{\partial \mathcal{L}_{\text{SSL}}(\theta; X_t)}{\partial \theta} \Big|_{\theta=\hat{\theta}(X_s)} \right) \frac{\partial \hat{\theta}(X_s)}{\partial (X_s)_{ij}}$$

By taking expectation and using the definition of the covariance,

$$\begin{aligned} \mathbb{E}_\zeta \left[\frac{\partial \mathcal{L}_{\text{SSL}}(\hat{\theta}(X_s); X_t)}{\partial (X_s)_{ij}} \right] &= \mathbb{E}_\zeta \left[\left(\frac{\partial \mathcal{L}_{\text{SSL}}(\theta; X_t)}{\partial \theta} \Big|_{\theta=\hat{\theta}(X_s)} \right) \frac{\partial \hat{\theta}(X_s)}{\partial (X_s)_{ij}} \right] \\ &= \mathbb{E}_\zeta \left[\sum_{k=1}^{d_\theta} \left(\frac{\partial \mathcal{L}_{\text{SSL}}(\theta; X_t)}{\partial \theta_k} \Big|_{\theta=\hat{\theta}(X_s)} \right) \frac{\partial \hat{\theta}(X_s)_k}{\partial (X_s)_{ij}} \right] \\ &= \sum_{k=1}^{d_\theta} \mathbb{E}_\zeta \left[\left(\frac{\partial \mathcal{L}_{\text{SSL}}(\theta; X_t)}{\partial \theta_k} \Big|_{\theta=\hat{\theta}(X_s)} \right) \frac{\partial \hat{\theta}(X_s)_k}{\partial (X_s)_{ij}} \right] \\ &= \sum_{k=1}^{d_\theta} \mathbb{E}_\zeta[v_k] \mathbb{E}_\zeta[\alpha_k] + \sum_{k=1}^{d_\theta} \text{Cov}_\zeta[v_k, \alpha_k], \end{aligned}$$

where $v_k = \frac{\partial \mathcal{L}_{\text{SSL}}(\theta; X_t)}{\partial \theta_k} \Big|_{\theta=\hat{\theta}(X_s)}$ and $\alpha_k = \frac{\partial \hat{\theta}(X_s)_k}{\partial (X_s)_{ij}}$. By defining the vectors $v = [v_1, v_2, \dots, v_{d_\theta}]^\top \in \mathbb{R}^{d_\theta}$ and $\alpha = [\alpha_1, \alpha_2, \dots, \alpha_{d_\theta}]^\top \in \mathbb{R}^{d_\theta}$,

$$\begin{aligned} \mathbb{E}_\zeta \left[\frac{\partial \mathcal{L}_{\text{SSL}}(\hat{\theta}(X_s); X_t)}{\partial (X_s)_{ij}} \right] &= \sum_{k=1}^{d_\theta} \mathbb{E}_\zeta[v_k] \mathbb{E}_\zeta[\alpha_k] + \sum_{k=1}^{d_\theta} \text{Cov}_\zeta[v_k, \alpha_k] \\ &= [\mathbb{E}_\zeta[v_1] \quad \dots \quad \mathbb{E}_\zeta[v_{d_\theta}]] \begin{bmatrix} \mathbb{E}_\zeta[\alpha_1] \\ \vdots \\ \mathbb{E}_\zeta[\alpha_{d_\theta}] \end{bmatrix} + \sum_{k=1}^{d_\theta} \text{Cov}_\zeta[v_k, \alpha_k] \\ &= \mathbb{E}_\zeta[[v_1 \quad \dots \quad v_{d_\theta}]] \mathbb{E}_\zeta \begin{bmatrix} \alpha_1 \\ \vdots \\ \alpha_{d_\theta} \end{bmatrix} + \sum_{k=1}^{d_\theta} \text{Cov}_\zeta[v_k, \alpha_k] \\ &= \mathbb{E}_\zeta[v]^\top \mathbb{E}_\zeta[\alpha] + \sum_{k=1}^{d_\theta} \text{Cov}_\zeta[v_k, \alpha_k]. \end{aligned}$$

Therefore, $\mathbb{E}_\zeta \left[\frac{\partial \mathcal{L}_{\text{SSL}}(\hat{\theta}(X_s); X_t)}{\partial (X_s)_{ij}} \right] = \mathbb{E}_\zeta[v]^\top \mathbb{E}_\zeta[\alpha] + \sum_{k=1}^{d_\theta} \text{Cov}_\zeta[v_k, \alpha_k]$. Comparing this with equation 7 proves the statement. \square

B VISUALIZATION OF DISTILLED IMAGES



Figure 3: Visualization of the synthetic images distilled by our method in CIFAR100.

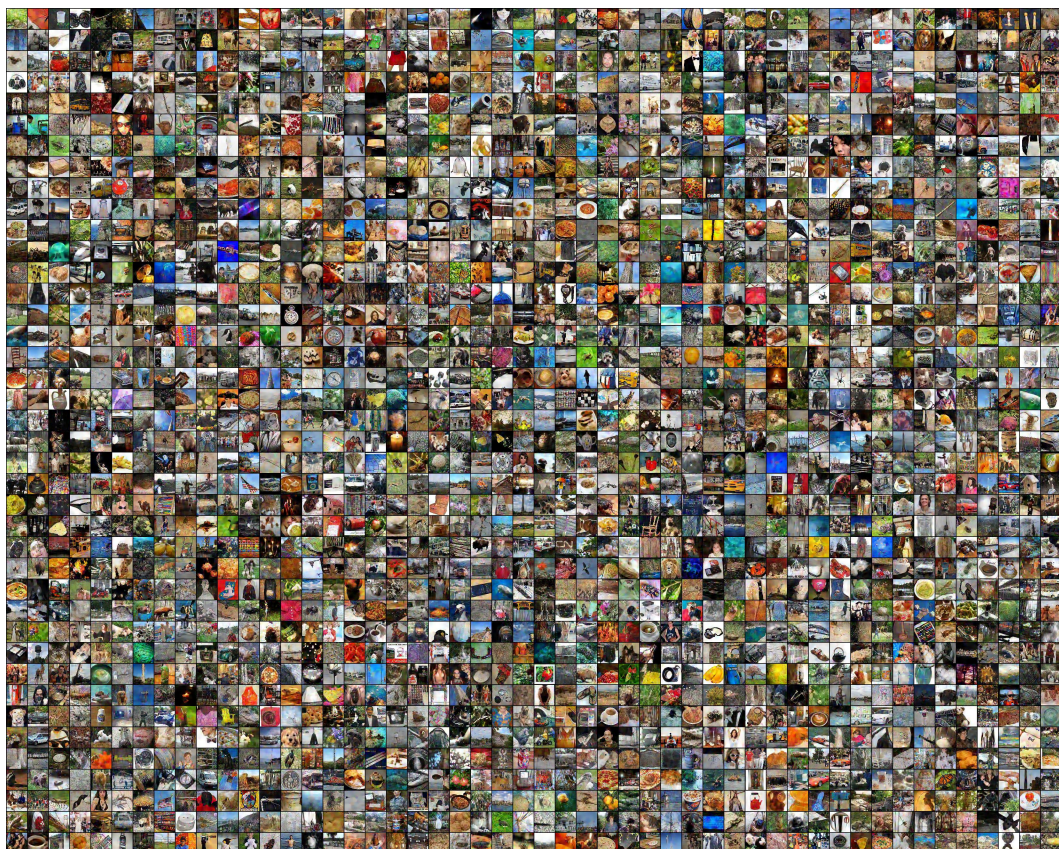


Figure 4: Visualization of the synthetic images distilled by our method in TinyImageNet.



Figure 5: Visualization of the synthetic images distilled by our method in ImageNet.

C ADDITIONAL EXPERIMENTAL RESULTS OF ARCHITECTURE GENERALIZATION

Table 6: The results of transfer learning using **VGG11**. Conv4 is utilized for condensing TinyImageNet into 2,000 synthetic examples. We report the average and standard deviation over three runs.

Method	Aircraft	Cars	CUB2011	Dogs	Flowers
w/o pre	35.73 ± 1.33	24.90 ± 0.67	27.75 ± 0.69	27.33 ± 0.39	56.46 ± 0.97
Random	32.72 ± 5.71	26.80 ± 0.70	27.10 ± 0.33	27.58 ± 0.43	60.11 ± 0.11
Kmeans	27.90 ± 14.60	28.13 ± 0.06	27.01 ± 0.68	28.28 ± 0.35	60.79 ± 0.54
DSA	34.22 ± 5.62	26.83 ± 0.50	27.24 ± 0.66	27.74 ± 0.51	61.01 ± 0.28
DM	38.78 ± 1.62	26.74 ± 0.21	27.09 ± 0.54	28.34 ± 0.08	60.78 ± 0.59
MTT	37.99 ± 3.39	34.80 ± 0.28	30.81 ± 0.37	32.41 ± 0.55	64.68 ± 0.26
FRePo	4.72 ± 0.84	31.37 ± 0.42	29.58 ± 0.20	29.86 ± 0.72	62.19 ± 0.88
KRR-ST	47.50 ± 2.09	52.78 ± 0.93	39.31 ± 0.12	39.10 ± 0.12	65.92 ± 0.29

Table 7: The results of transfer learning using **AlexNet**. Conv4 is utilized for condensing TinyImageNet into 2,000 synthetic examples. We report the average and standard deviation over three runs.

Method	Aircraft	Cars	CUB2011	Dogs	Flowers
w/o pre	29.30 ± 6.56	18.38 ± 0.12	21.52 ± 0.22	21.91 ± 0.12	51.88 ± 0.32
Random	8.24 ± 2.68	19.19 ± 0.20	21.42 ± 0.41	17.51 ± 1.81	46.06 ± 3.96
Kmeans	4.15 ± 0.70	20.47 ± 0.31	21.66 ± 0.31	19.03 ± 1.80	52.24 ± 1.71
DSA	3.64 ± 1.66	20.40 ± 0.40	21.63 ± 0.49	21.06 ± 0.95	54.59 ± 0.77
DM	10.53 ± 5.85	18.76 ± 0.30	20.32 ± 0.49	20.36 ± 0.17	51.75 ± 0.95
MTT	10.79 ± 6.34	24.45 ± 0.47	24.63 ± 0.50	23.81 ± 0.46	56.73 ± 0.15
FRePo	37.33 ± 1.88	28.33 ± 0.81	25.90 ± 0.47	24.66 ± 0.69	60.09 ± 0.67
KRR-ST	49.25 ± 0.70	38.20 ± 1.26	31.52 ± 0.82	30.49 ± 0.46	64.51 ± 0.94

Table 8: The results of transfer learning using **MobileNet**. Conv4 is utilized for condensing TinyImageNet into 2,000 synthetic examples. We report the average and standard deviation over three runs.

Method	Aircraft	Cars	CUB2011	Dogs	Flowers
w/o pre	6.61 ± 0.46	3.94 ± 0.34	4.94 ± 0.35	9.28 ± 0.17	10.39 ± 2.26
Random	31.14 ± 2.11	16.12 ± 1.16	18.38 ± 0.69	20.44 ± 0.75	43.65 ± 1.13
Kmeans	31.99 ± 0.72	19.31 ± 1.25	18.86 ± 0.32	22.37 ± 0.72	42.72 ± 1.06
DSA	29.41 ± 1.36	16.68 ± 1.12	18.70 ± 1.71	21.34 ± 0.90	44.45 ± 0.63
DM	35.89 ± 0.91	19.94 ± 0.70	19.74 ± 1.89	23.03 ± 0.49	42.60 ± 2.06
MTT	34.92 ± 0.77	21.71 ± 0.07	22.15 ± 0.84	27.04 ± 0.44	45.21 ± 0.38
FRePo	25.00 ± 0.43	15.51 ± 0.34	20.20 ± 0.63	22.75 ± 0.57	41.07 ± 0.98
KRR-ST	33.01 ± 1.23	38.81 ± 0.91	24.96 ± 0.99	39.10 ± 0.28	46.64 ± 1.15

Table 9: The results of transfer learning using **ResNet10**. Conv4 is utilized for condensing TinyImageNet into 2,000 synthetic examples. We report the average and standard deviation over three runs.

Method	Aircraft	Cars	CUB2011	Dogs	Flowers
w/o pre	3.69 ± 0.18	2.43 ± 0.08	2.33 ± 0.07	3.03 ± 0.16	12.57 ± 0.37
Random	11.86 ± 0.45	8.76 ± 0.22	7.62 ± 0.06	16.05 ± 0.46	39.44 ± 0.97
Kmeans	13.17 ± 0.15	9.62 ± 0.17	7.62 ± 0.34	17.18 ± 0.25	40.68 ± 0.38
DSA	13.94 ± 0.92	9.14 ± 0.44	9.44 ± 0.21	17.24 ± 0.41	41.22 ± 0.60
DM	13.90 ± 0.13	9.46 ± 0.46	8.97 ± 0.16	17.56 ± 0.23	41.37 ± 0.37
MTT	15.43 ± 0.08	10.80 ± 0.28	10.67 ± 0.15	19.49 ± 0.61	43.95 ± 0.04
FRePo	4.18 ± 0.14	2.23 ± 0.24	2.97 ± 0.18	6.63 ± 0.27	9.32 ± 0.98
KRR-ST	27.29 ± 0.88	21.41 ± 1.31	13.97 ± 0.98	31.83 ± 0.86	39.75 ± 1.49